Control of traveling-wave oscillations and bifurcation behavior in central pattern generators

Control of traveling-wave oscillations and bifurcation behavior in central pattern generators

Alexandra S. Landsman[1,*] and Jean-Jacques Slotine[2,†]
[1]*Physics Department, ETH Zurich, CH-8093 Zurich, Switzerland*
[2]*Nonlinear Systems and Brain Sciences Laboratory, MIT, Cambridge, Massachusetts 02139, USA*
(Received 29 May 2012; published 23 October 2012)

Understanding synchronous and traveling-wave oscillations, particularly as they relate to transitions between different types of behavior, is a central problem in modeling biological systems. Here, we address this problem in the context of central pattern generators (CPGs). We use contraction theory to establish the global stability of a traveling-wave or synchronous oscillation, determined by the type of coupling. This opens the door to better design of coupling architectures to create the desired type of stable oscillations. We then use coupling that is both amplitude and phase dependent to create either globally stable synchronous or traveling-wave solutions. Using the CPG motor neuron network of a leech as an example, we show that while both traveling and synchronous oscillations can be achieved by several types of coupling, the transition between different types of behavior is dictated by a specific coupling architecture. In particular, it is only the "repulsive" but not the commonly used phase or rotational coupling that can explain the transition to high-frequency synchronous oscillations that have been observed in the heartbeat pattern generator of a leech. This shows that the overall dynamics of a CPG can be highly sensitive to the type of coupling used, even for coupling architectures that are widely believed to produce the same qualitative behavior.

DOI: 10.1103/PhysRevE.86.041914 PACS number(s): 87.10.Ed, 05.45.Xt, 87.10.Ca

I. INTRODUCTION

Coupled limit cycle oscillators are used to model many physical phenomena in biology and engineering. While most prior studies have focused on synchronous oscillations, there has been a growing interest in traveling-wave oscillations, particularly in the context of central pattern generators (CPGs). These are neural circuits found in both vertebrate and invertebrate animals that can produce rhythmic patterns of activity without an external periodic drive. CPGs are fundamental to many periodic activities such as chewing, moving, and breathing and have inspired many robotic models of animal and even human locomotion [1–4]. The advantages of using CPGs to model locomotion in robots include [5] (i) the use of limit cycle behavior to produce stable periodic patterns, (ii) suitability for distributed implementation [6], and (iii) few control parameters, which allows for the modulation of locomotion [1].

A central problem in modeling CPGs using coupled limit cycle oscillators is finding and proving the stability of solutions that correspond to relevant phenomena, such as, for instance, different types of gait in animal locomotion. While it has been shown that it is possible to find solutions using spatiotemporal symmetries of the model [7], proving global stability of these solutions remains one of the central problems in CPG design and implementation [5]. Much work has been done showing stability of synchronous solutions (see, for example, Ref. [8] for a review). In this case, it is possible to prove local stability by linearizing around the synchronous state [9]. A particular challenge is proving global stability of out-of-phase oscillations. These oscillations model the traveling wave of electrical activity that is behind undulatory swimming.

In this work, we show that contraction theory [10] can be used to establish the global stability of a traveling wave, allowing more effective design of traveling waves of controlled amplitude, as well as synchronous oscillations. In a recent paper, a traveling wave generated by a double chain of oscillatory centers (representing groups of neurons on the two sides of the spinal cord) has been shown to be involved in both the swimming and walking behavior of a salamander [1]. Some work has been done in proving the stability of a traveling-wave solution in phase-coupled oscillators [3,11]. Phase coupling (which has no dependence on the amplitude of the oscillations) is frequently used to model weakly coupled limit cycle oscillators [12], where the dynamics is assumed to remain on a limit cycle. However, it has been shown that in weakly coupled cortical neurons off-limit-cycle dynamics contributes to synchronization by modulating the period of oscillation [13].

In the lamprey and salamander, both phase and amplitude dependence in coupling is needed to produce three different phases of the dynamics [1,14] corresponding to (i) a subthreshold phase without bursts, (ii) a bursting phase, with the frequency and amplitude of the bursts dependent on the drive, and (iii) a saturation phase, where no oscillations occur. Here, we give an example of three analogous types of dynamics in a leech, demonstrating that in this case as well, both amplitude and phase dependence in coupling are needed to account for the dynamics. The combined results suggest that the commonly used phase coupling may not be sufficient to model many CPG systems of interest.

Rotational coupling, which has both a phase and an amplitude dependence, has been previously shown to generate a stable traveling wave in nearest-neighbor coupled oscillators [15,16]. Here, we use phase- and amplitude-dependent inhibitory (repulsive) coupling to achieve a similar effect in a more physical way, in essence allowing the system itself to compute the couplings achieving the out-of-phase behavior.

*landsmaa@phys.ethz.ch
†jjs@mit.edu

Our basic model consists of a chain of nearest-neighbor coupled Andronov-Hopf limit cycle oscillators, whereby the nth oscillator is connected to the first oscillator in a ring structure. The system is given by

$$\dot{\mathbf{x}}_j = \mathbf{F}(\mathbf{x}_j) + k(\mathbf{x}_j - \mathbf{x}_{j+1} - \mathbf{x}_{j-1}), \tag{1}$$

where $\mathbf{x}_j = \{x_j, y_j\}$ is a two-dimensional vector describing the dynamics of the jth oscillator, with $\mathbf{F}(\mathbf{x})$ given by

$$\mathbf{F}\begin{pmatrix} x \\ y \end{pmatrix} = \begin{pmatrix} \alpha x - \omega y - x^3 - xy^2 \\ \omega x + \alpha y - y^3 - yx^2 \end{pmatrix}. \tag{2}$$

Due to symmetry considerations [7], the synchronous state is one possible solution to the above equation, resulting in an amplitude of oscillation given by $|\mathbf{x}_j| = \sqrt{\alpha + |k|}$. This solution will be shown in the next section to be globally stable for diffusive types of coupling, given by $k < 0$. For repulsive coupling, given by $k > 0$, the system tends to an out-of-phase state, whereby the neighboring oscillators are maximally out of phase with each other [17]. This results in two different types of dynamics, depending on whether the number of oscillators, N, is even or odd. When N is even, the array oscillates with a difference of π between nearest neighbors, splitting into two equal synchronous groups that are 180° out of phase with each other (see Fig. 1, plotted for $N = 4$). The phase difference between nearest neighbors is thereby given by

$$\Delta\,\phi^{\text{even}}_{j,j+1} = \pi. \tag{3}$$

A traveling-wave solution is possible when the number of oscillators is odd. Requiring the neighboring oscillators to be maximally out of phase while preserving the symmetry of the system leads to two possible degenerate solutions given by

$$\Delta\phi^{\text{odd}}_{j,j+1} = \pi \pm \pi/N. \tag{4}$$

The smallest phase difference between the two oscillators is given by the next-to-nearest-neighbor phase difference: $\Delta\phi^{\text{odd}}_{j,j+2} \pm 2\pi/N$. The vectors $\mathbf{x}_j$ therefore fall on a circle

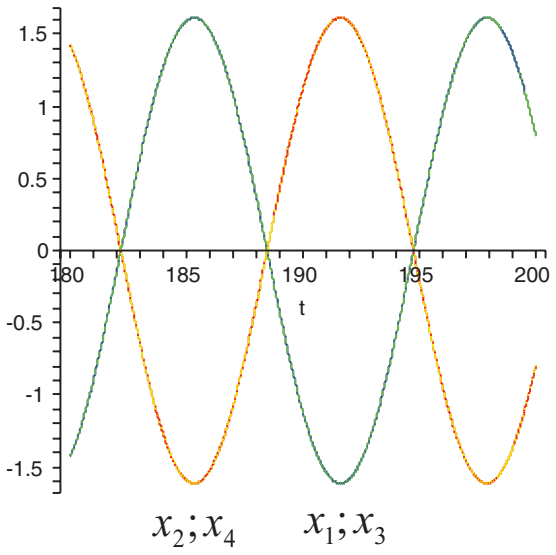

FIG. 1. (Color online) Symmetric solution for a repulsively coupled array, $k > 0$, for an even number of oscillators, $N = 4$, $\alpha = 1$, $k = 0.11$. The figure shows that the neighboring oscillators are maximally out of phase.

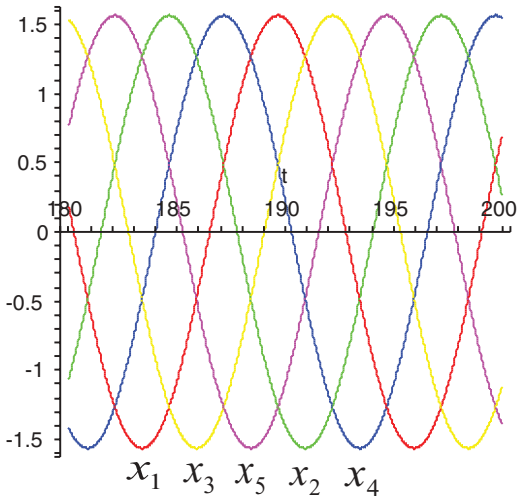

FIG. 2. (Color online) Traveling-wave solution for repulsively coupled array for an odd number of oscillators, $N = 5$, $\alpha = 1$, $k = 0.11$. The neighboring oscillators are out of phase by $\pi + \pi/5$ (for example, compare the first and the second oscillators).

where they are spaced with an equal phase difference of $2\pi/N$, forming a symmetric out-of-phase solution.

Figure 2 illustrates the stable out-of-phase dynamics for $N = 5$, where each oscillator is shifted in phase from its neighbor by $\pi + \pi/5$.

To solve for the amplitude of the out-of-phase solution for N even and N odd, we use Eqs. (3) and (4), respectively, and substitute these solutions for the nearest-neighbor terms into Eq. (1), resulting in

$$|\mathbf{x}_j|^{N_{\text{odd}}} = \{\alpha + k[(1 + 2\cos(\pi/N)]\}^{1/2}, \tag{5}$$

$$|\mathbf{x_j}|^{N_{\text{even}}} = (\alpha + 3k)^{1/2}. \tag{6}$$

Note that in Eq. (6), the amplitude of the oscillation is independent of the total number of oscillators, while in the traveling-wave amplitude, given by Eq. (5), it increases with increasing N, asymptotically approaching $(\alpha + 3k)^{1/2}$ as $n \to \infty$.

We now prove the global stability of the synchronous and traveling-wave solutions when $k < 0$ and $k > 0$, respectively, for the $N = 3$ case (it is straightforward to extend our approach to higher N). While our results are limited to nominally identical oscillators, they are robust to variations in individual parameters and the associated deviations from the ideal case can be explicitly quantified [15,18]. For nonidentical frequencies, the stability of phase-locked solutions is determined by Arnold tongues [8] that set an upper bound on the possible variation in the frequency of individual oscillators as a function of the coupling strength. Therefore, our analysis should be robust to variation of the parameters, as long as the coupling is sufficiently strong to overcome the spread in frequencies of nonidentical oscillators.

A sufficient condition for global exponential stability on a flow-invariant linear subspace $\mathcal{M}$ [i.e., a linear subspace $\mathcal{M}$ such that $\forall\, t : \mathbf{F}(\mathcal{M},t) \subset \mathcal{M}$] as given by [15]

$$-\lambda_{\min}(\mathbf{V}\mathbf{L}\mathbf{V}^T) > \sup \lambda_{\max}\left(\frac{\partial \mathbf{F}}{\partial \mathbf{x}}\right), \tag{7}$$

where $\mathbf{V}$ forms a basis of the linear subspace $\mathcal{M}^{\perp}$ (orthogonal to $\mathcal{M}$), $\partial\mathbf{F}/\partial\mathbf{x}$ is the Jacobian of the uncoupled system, with $\mathbf{F}$ given by Eq. (2), and $\mathbf{L}$ is the coupling matrix, to be given below. The terms $\lambda_{\min}$ and $\lambda_{\max}$ indicate the minimum and maximum eigenvalues of the symmetric parts of the matrices $\mathbf{L}$ and $\partial\mathbf{F}/\partial\mathbf{x}$, respectively. Intuitively, the above condition ensures that the system is contracting in the orthogonal subspace $\mathcal{M}^{\perp}$, thereby ensuring that the dynamics converges exponentially to $\mathcal{M}$.

From Eq. (1), the coupling matrix $\mathbf{L}$ for the $N = 3$ case is given by

$$\mathbf{L} = \mathbf{k}\begin{pmatrix} I & -I & -I \\ -I & I & -I \\ -I & -I & I \end{pmatrix}, \tag{8}$$

where I above is a 2×2 identity matrix. The entire phase space $\mathcal{M} \oplus \mathcal{M}^{\perp}$ is spanned by a total of six vectors: the two vectors spanning the synchronous solution, plus the four vectors spanning a linear vector subspace formed by the two degenerate out-of-phase solutions. For convenience, let us define the subspace corresponding to the synchronous case as

$$\mathcal{M}_{\text{sync}} = \{(\mathbf{x},\mathbf{x},\mathbf{x}) : \mathbf{x} \in \mathcal{R}^{\mathbf{2}}\} \tag{9}$$

and the subspace corresponding to the out-of-phase states as

$$\mathcal{M}_{\text{phase}} = \{(\mathbf{x},\mathbf{R}_{2\pi/3}\mathbf{x},\mathbf{R}_{4\pi/3}\mathbf{x}),(\mathbf{x},\mathbf{R}_{4\pi/3}\mathbf{x},\mathbf{R}_{2\pi/3}\mathbf{x})\}, \tag{10}$$

where $\mathbf{R}$ is a 2×2 rotation matrix, with the rotation angles of $\{2\pi/3,4\pi/3\}$ obtained from Eq. (4) for the $N = 3$ case. The corresponding eigenvectors can be obtained by substituting $\mathbf{x} = \{1,0\}$ and $\{0,1\}$ into Eqs. (9) and (10), resulting in six orthogonal eigenvectors. In complex form the two out-of-phase solutions given in Eq. (10) can also be written as $z(1,e^{i2\pi/3},e^{i4\pi/3})$ and $z(1,e^{i4\pi/3},e^{i2\pi/3})$. As before, the entire phase space of solutions is spanned by the sum $\mathcal{M}_{\text{sync}} \oplus \mathcal{M}_{\text{phase}}$.

Having obtained all the eigenvectors, we can now use Eq. (7) to analyze the stability of either the synchronous or the out-of-phase states, represented by $\mathcal{M}_{\text{sync}}$ and $\mathcal{M}_{\text{phase}}$, respectively. As will be shown shortly, this stability depends on the value of the coupling constant k, with the synchronous solution being stable for negative k (or a diffusive type of coupling) and the out-of-phase subspace being stable for positive values of k (representing repulsive coupling).

To analyze the stability of the synchronous state, we equate $\mathcal{M}_{\text{sync}} \equiv \mathcal{M}$ and $\mathcal{M}_{\text{phase}} \equiv \mathcal{M}^{\perp}$, thereby obtaining the 6×4 matrix $\mathbf{V}$ from Eq. (10). The four eigenvalues of $\mathbf{VLV}^T$, with $\mathbf{L}$ given in Eq. (8), are all identical and given by $\lambda_{1,2,3,4} = 2k$. The eigenvalues of the symmetric part of the Jacobian, $\partial\mathbf{F}/\partial\mathbf{x}$, are given by $\alpha - |x|^2$ and $\alpha - 3|x|^2$, which are upper-bounded by α. It follows from Eq. (7) that the solution converges exponentially to $\mathcal{M}_{\text{sync}}$ when

$$k < -\alpha/2. \tag{11}$$

Next, doing the reverse by equating $\mathcal{M}_{\text{phase}} \equiv \mathcal{M}$ and $\mathcal{M}_{\text{sync}} \equiv \mathcal{M}^{\perp}$, we again obtain the eigenvalues of $\mathbf{VLV}^T$ [with $\mathbf{V}$ now given by Eq. (9)]: $\lambda_{5,6} = -k$. Combining the above results and again using Eq. (7), we now get the condition for the global stability of $\mathcal{M}_{\text{phase}}$:

$$k > \alpha. \tag{12}$$

Equations (11) and (12) give conditions for the global stability of synchronous and traveling-wave solutions, respectively.

We now compare the model in Eq. (1), which has repulsive coupling, given by $k > 0$, to an alternative way of generating a globally stable traveling wave using either (a) rotational or (b) phase coupling. For rotational coupling, Eq. (1) becomes

$$\dot{\mathbf{x}}_j = \mathbf{F}(\mathbf{x}_j) + k(\mathbf{x}_j - \mathbf{R}_{2\pi/N}\mathbf{x}_{j-1}). \tag{13}$$

While the rotational coupling given in Eq. (13) also produces a globally stable traveling wave [15,16], there are important differences in dynamics, including the following: (I) The existence of an out-of-phase solution for any number N of oscillators. This is in contrast to the system analyzed here, where an odd N is needed for an out-of-phase state. (II) The existence of a single (nondegenerate) out-of-phase solution, unlike the two solutions given in Eq. (10). (III) Different phase differences between nearest neighbors. Thus, the phase difference given by Eq. (4) is such that the nearest neighbors are maximally out of phase, while the phase difference from rotational coupling is such that oscillator j is advanced from $j - 1$ by a phase of $2\pi/N$. (IV) With rotational coupling, the amplitude of the oscillation is preserved, as compared to the uncoupled case. This can be seen by directly substituting the out-of-phase solution $\mathbf{x}_j = \mathbf{R}_{2\pi/N}\mathbf{x}_{j-1}$ into Eq. (13), whereby the coupling term drops out. In contrast, in the repulsive coupling, the amplitude of the traveling wave increases with the coupling constant, as can be seen from Eq. (5). Similarly, for phase coupling, the amplitude of oscillation is independent of the coupling, since the dynamics is assumed to remain on the limit cycle.

Here, we present an example where, due to property IV (i.e., the amplitude increase of a traveling wave), only repulsive but not phase or rotational coupling can explain an important qualitative change in behavior.

Example. The heartbeat pattern generator of a medicinal leech consists of two groups of neurons coupled together by a common element (namely, interneurons located in ganglion 5 [19]). The first group are called oscillator interneurons; they form mutually inhibitory synapses with each other. The second group, called premotor heart interneurons, have excitatory synapses. These two arrays are known to correspond to two types of motion: a traveling wave that beats in a rear to front (peristaltic) fashion, and a synchronous state.

It has been suggested [20] that this network can be represented by two globally coupled arrays: one with inhibitory (repulsive) coupling, corresponding to oscillator interneurons, and another one with local diffusive (excitatory) coupling, representing premotor heart interneurons. The global interaction term corresponds to the mutual coupling of the two arrays via ganglion 5, and depends on the overall activity of the two arrays.

The overall topology of this network is shown in Fig. 3, with dynamics represented by the following set of equations:

$$\dot{\mathbf{x}}_j^r = \mathbf{F}\left(\mathbf{x}_j^r\right) + k_l\left(\mathbf{x}_j^r - \mathbf{x}_{j+1}^r - \mathbf{x}_{j-1}^r\right) + c\sum_{k=1}^{N}\left|\mathbf{x}_k^d\right|, \tag{14}$$

$$\dot{\mathbf{x}}_j^d = \mathbf{F}\left(\mathbf{x}_j^d\right) - k_l\left(\mathbf{x}_j^d - \mathbf{x}_{j+1}^d - \mathbf{x}_{j-1}^d\right) + c\sum_{k=1}^{N}\left|\mathbf{x}_k^r\right|, \tag{15}$$

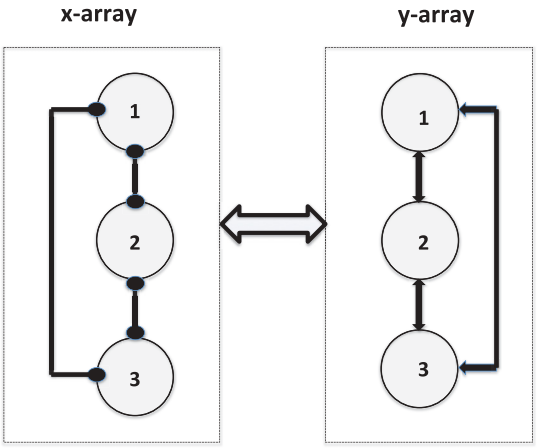

FIG. 3. Topology of the network described by Eqs. (14) and (15) for the $N = 3$ case. The x array corresponds to oscillator interneurons, with mutually inhibitory (repulsive) local coupling, represented by connections with filled-in ovals. The y array corresponds to the premotor heart neurons, with excitatory (diffusive) local connections, shown by solid black arrows. The two arrays are globally coupled to each other, with the strength of the coupling given by c and dependent on the overall activity of the two arrays.

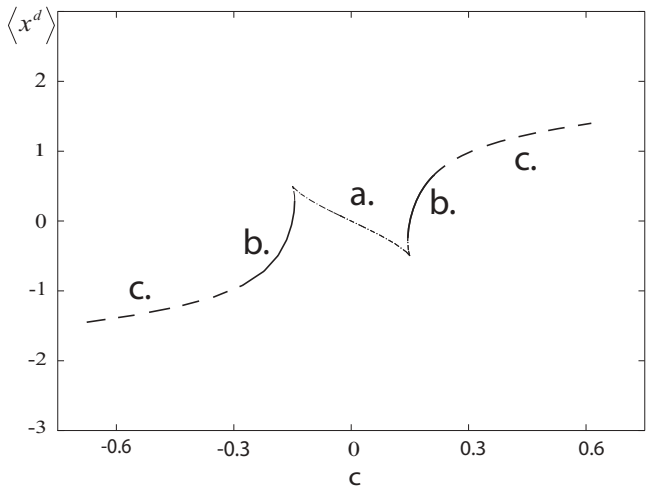

FIG. 4. Bifurcation diagram as a function of the global coupling constant c for a system given by Eqs. (14) and (15), $\alpha = 1$, $k_l = 0.2$, $\omega = 1/2, N = 3$. a. $|c| < c_{\text{bif}}$. Both arrays oscillate at frequency ω. b. $c_{\text{bif}} < |c| < \tilde{c}_{\text{bif}}$. High-frequency, $N\omega$, oscillations, which correspond to experimentally observed bursting behavior, occur in the diffusively coupled array. c. $|c| > \tilde{c}_{\text{bif}}$. Oscillator death.

where $k_l > 0$, $\mathbf{F}(\mathbf{x})$ is defined in Eq. (2), and N is the number of oscillators in each array. The superscripts r and d denote repulsively and diffusively coupled arrays, respectively. Note that in the absence of global coupling, $c = 0$, Eqs. (14) and (15) are the same as Eq. (1). Therefore for small c, Eq. (14) generates a stable traveling wave (corresponding to peristaltic motion), while Eq. (15) has a stable synchronous state, oscillating at frequency ω.

It was experimentally demonstrated [19] that the bursting in a leech occurs within a narrow range of parameters, corresponding to a bifurcation. This narrow range is separated on either side by zones of tonic spiking or silence. As the global coupling strength c between the two arrays is increased, an onset of high-frequency, $N\omega$, oscillations is observed in a diffusively coupled array, at a bifurcation value given by $c = c_{\text{bif}}$ [20,21], as shown in Fig. 4. Note that this onset corresponds to this experimentally observed transition from tonic spiking to bursting [19].

It was shown in Ref. [17] that the bifurcation value for globally coupled limit cycle arrays can be calculated by replacing the global coupling term $c\sum_{k=1}^{N}|\mathbf{x}_k|$ with $cN|\mathbf{x}_0|$, where $|\mathbf{x}_0|$ is the amplitude of the corresponding stable solution in the absence of global coupling. The bifurcation values for the two arrays are then given by $c_{\text{bif}} = C_b/N|\mathbf{x}_0^r|$ and $\tilde{c}_{\text{bif}} = \tilde{C}_b/N|\mathbf{x}_0^d|$, where c_{bif} and $\tilde{c}_{\text{bif}}$ correspond to a bifurcation for diffusively and repulsively coupled arrays, respectively. The bifurcation constants C_b and $\tilde{C}_b$ can be found by calculating when the three real roots of the intersection of the $\dot{x} = 0$ nullcline with a vertical line disappear [22], resulting in

$$C_b = \frac{(8\gamma^2 + \omega^2)}{4\gamma^{1/2}}, \qquad \tilde{C}_b = \frac{(8\tilde{\gamma}^2 + \omega^2)}{4\tilde{\gamma}^{1/2}}, \tag{16}$$

where $\gamma = (\alpha + k_l)/3$ and $\tilde{\gamma} = \{\alpha + k_l[1 + 2\cos(\pi/N)]\}/3$. Using Eq. (16) and substituting into c_{bif} and $\tilde{c}_{\text{bif}}$, as well as using the amplitudes of the steady-state oscillations for the diffusively and repulsively coupled arrays, given by $|\mathbf{x}_0^d| = (3\gamma)^{1/2}$ and $|\mathbf{x}_0^r| = (3\tilde{\gamma})^{1/2}$ [see Eq. (5)], we get

$$c_{\text{bif}} = \frac{8\gamma^2 + \omega^2}{4N\sqrt{3\gamma\tilde{\gamma}}}, \qquad \tilde{c}_{\text{bif}} = \frac{8\tilde{\gamma}^2 + \omega^2}{4N\sqrt{3\gamma\tilde{\gamma}}}, \tag{17}$$

where $\tilde{c}_{\text{bif}} > c_{\text{bif}}$, since $\tilde{\gamma} > \gamma$. An onset of high-frequency, $N\omega$, oscillation is observed for a global coupling constant in the range

$$c_{\text{bif}} < c < \tilde{c}_{\text{bif}}. \tag{18}$$

For $c < c_{\text{bif}}$, both diffusively and repulsively coupled arrays oscillate at frequency ω, synchronously and out of phase, respectively, while oscillator death occurs for $c > \tilde{c}_{\text{bif}}$ (see Fig. 3).

In contrast, there is no range of the global coupling constant for which high-frequency oscillations are observed if the traveling wave is created by rotational rather than repulsive coupling. This corresponds to replacing the nearest-neighbor coupling term in Eq. (14) by the rotational coupling term given by Eq. (13). In this case $|\mathbf{x}_0^d|$, and therefore γ, remains the same. However, $|\mathbf{x}_0^r|$ is now obtained by solving $\dot{\mathbf{x}} = \mathbf{F}(\mathbf{x})$, since the rotational coupling term drops out in a steady state forming a traveling wave, resulting in $|\mathbf{x}_0^r| = \sqrt{\alpha}$ and $\tilde{\gamma} = \alpha/3$. Since in this case $c_{\text{bif}} > \tilde{c}_{\text{bif}}$, there is no range of c for which Eq. (18) is satisfied and the onset of high-frequency oscillations does not occur.

For phase coupling the amplitudes of both out-of-phase and synchronous oscillations are the same, irrespective of the coupling topology, since the dynamics is assumed to remain on the limit cycle due to the weakness of connections, resulting in $\gamma = \tilde{\gamma}$. Again, in this case Eq. (18) is not satisfied for any value of c and either both arrays oscillate at frequency ω or oscillator death occurs if $c > c_{\text{bif}}$ [23].

In conclusion, contraction theory was used to establish the stability of our network designs using either diffusive or repulsive coupling and yet with both phase and amplitude

dependence. Recent work has shown that such dependence is needed to explain the different phases of the dynamics in a salamander and in a lamprey [1]. We show that, similarly, this more complicated form of coupling (as compared to only phase coupling) is also needed to account for the three different types of dynamics in a very different model of a leech heartbeat. The results suggest that phase oscillators, although very common in modeling neural networks, may nevertheless be insufficient to model many CPGs of interest.

We also considered two types of phase- and amplitude-dependent coupling, namely, rotational and mutually inhibitory (repulsive) coupling. In nature, very few examples of rotational coupling, as compared to inhibitory coupling, exist. Unlike rotational coupling, inhibitory coupling does not require a precise phase difference and therefore is much more robust to perturbations. We showed using contraction theory that inhibitory coupling can also create a stable traveling wave, similar to the one created by rotational coupling. This suggests that inhibitory coupling is a better and a more biologically plausible alternative in designing traveling waves that commonly occur in CPGs.

Our results also suggest that arrays that use phase- and amplitude-dependent inhibitory and excitatory coupling can be combined to design biologically inspired models of CPGs. We demonstrate by analyzing a model of a leech heartbeat, showing that by combining these two types of arrays one can account analytically for certain essential features of experimentally observed dynamics.

A.S.L. acknowledges support from a Marie Curie International Incoming Grant within the FP7 Framework.

[1] A. J. Ijspeert, A. Crespi, D. Ryczko, and J. M. Cabelguen, Science **315**, 5817 (2007).
[2] S. Aoi and K. Tsuchiya, Autonomous Robots **19**, 219 (2005).
[3] G. B. Ermentrout and N. Kopell, SIAM J. Appl. Math. **54(2)**, 478 (1994).
[4] L. Righetti and A. J. Ijspeert, in *Proceedings of the IEEE International Conference on Robotics and Automation*, edited by S. Hutchinson (IEEE Robotics and Automation, Orlando, FL, 2006).
[5] L. J. Ijspeert, Neural Networks **21**, 642 (2008).
[6] J. Conradt, and P. Varshavskaya, *in Proceedings of the International Conference on Artificial Neural Networks*, edited by O. Kaynak (Springer, New York, 2003).
[7] M. Golubitsky, I. Stewart, P. L. Buono, and J. J. Collins, Nature (London) **401**, 693 (1999).
[8] A. Pikovsky, M. Rosenblum, and J. Kurths, *Synchronization: A Universal Concept in Nonlinear Science* (Cambridge University Press, Cambridge, 2003).
[9] L. M. Pecora and T. L. Carroll, Phys. Rev. Lett. **64**, 821 (1990).
[10] W. Lohmiller and J. J. E. Slotine, Automatica **34**, 683 (1998).
[11] N. Kopell and G. B. Ermentrout, Commun. Pure Appl. Math. **39**, 623 (1986).
[12] F. C. Hoppensteadt and E. M. Izhikevich, *Weakly Connected Neural Networks* (Springer, New York, 1997).
[13] A. S. Landsman and I. B. Schwartz, Nonlinear Biomed. Phys. **1**, 2 (2007).
[14] J. M. Cabelguen, C. Bourcier-Lucas, and J. Dubuc, J. Neurosci. **23**, 2434 (2003).
[15] Q. C. Pham and J. J. Slotine, Neural Networks **20**, 1 (2007).
[16] K. Seo and J. J. Slotine, in *Proceedings of the IEEE International Conference on Robotics and Automation*, edited by S. Hutchinson (IEEE Robotics and Automation, Rome, 2007), p. 281.
[17] A. S. Landsman and I. B. Schwartz, Phys. Rev. E **74**, 036204 (2006).
[18] N. Tabareau, J. J. E. Slotine, and Q. C. Pham, PLoS Comput. Biol. **6**, 1 (2010).
[19] G. S. Cymbalyuk, Q. Gaudry, M. A. Masino, and R. L. Calabrese, J. Neurosci. **22**, 10580 (2002).
[20] P. L. Buono and A. Palacios, Physica D **188**, 292 (2004).
[21] A. Palacios, R. Carretero-Gonzalez, P. Longhini, N. Renz, V. In, A. Kho, J. D. Neff, B. K. Meadows, and A. R. Bulsara, Phys. Rev. E **72**, 026211 (2005).
[22] J. Guckenheimer and P. Holmes, *Nonlinear Oscillations, Dynamical Systems and Bifurcations of Vector Fields* (Springer-Verlag, New York, 1983), Vol. 2.
[23] D. G. Aronson, G. B. Ermentrout, and N. Koppel, Physica D **41**, 403 (1990).